Tuijin Jishu/Journal of Propulsion Technology
ISSN: 1001-4055
Vol. 45 No.1 (2024)

Design Evaluation of Wireless Ultra-Fast Charging System and Related Thermal Management System for Electric Vehicles

Joyashree Das[1*], Sumit Sarkar[2] and Sharmistha Sharma[1]

[1]*Faculty of Electrical Engineering, National Institute of Technology Agartala, Agartala, Tripura, India*

[2]*B Tech scholar of Electrical Engineering, National Institute of Technology Agartala, Agartala, Tripura, India*

Abstract: - As the use of Electrical Vehicles has become a more sustainable option over the past decade, innovation is needed to make Electrical Vehicles more accessible. Fast charging is a widely used Electrical Vehicle charging method, but ultra-fast charging has been studied to a limited extent. One of the main research areas is improving loading speed and time. This paper presents a detailed implementation of the Simulink models of fast charging and ultra-fast charging, along with the associated thermal management system. All the necessary calculations and schematics and a comparison of fast charging and ultra-fast charging have been performed. The graphs between SOC (state of charge) and charging time is obtained for both the fast-charging model and the ultra-fast charging model. It is observed that the slope of the ultra-fast charging model is larger than that of the fast-charging model. Therefore, with the same charging time, the battery charges more in the ultra-fast charging model.

Keywords: *Wireless ultra-fast charging system, Thermal management system, Electric vehicles.*

1. Introduction

An electric vehicle is a means of transportation powered by an electric motor connected to the wheels. Electric vehicles have low running costs due to fewer moving parts to maintain and are very environmentally friendly as it uses little or no fossil fuels (gasoline or diesel) [1]. Some electric vehicles used lead-acid or nickel-metal hydride batteries, but today's lithium-ion batteries have a long life and excellent energy storage capabilities with a self-discharge rate of only 5%. It is considered the standard for modern battery electric vehicles day by day [2]. Despite these efficiency improvements, these batteries still have challenges. Despite efforts to improve the safety of these batteries, it can still experience thermal runaway, which has caused fires and explosions in Tesla models, for example. Thermal management system.

Ultimately, the components must operate in their optimum temperature range while producing a comfortable temperature for the occupants inside the vehicle. In general, the thermal management system for electric vehicles is more complex than for conventional vehicles with internal combustion engines. For example, the e-axle always needs to be cooled, while the battery needs to be cooled or heated depending on the situation [3]. Furthermore, waste heat from the internal combustion engine cannot be used to heat the passenger compartment with the required heat pump. Refrigerant and cooling circuits must be optimally coordinated to transport heat within the vehicle and provide the required temperatures. The interconnection of these two circuits will change depending on the heating or cooling requirements. This gives rise to different modes of operation.

Coolant is circulated by a pump in the cooling circuit. Coolant moves from where heat is generated to where it is needed inside the vehicle. Due to its high specific heat capacity, the coolant can absorb a large amount of heat in a very small space. This is necessary for the effective cooling of e-axles, batteries, etc [4,10,11]. With coolant, the heat distribution within the vehicle is also very flexible. As the coolant absorbs heat, its

temperature rises, so it must be cooled with a heat exchanger.

Liquid or gas refrigerant circulates in the refrigerant circuit. Evaporation of the refrigerant (transition from liquid to gas) creates refrigeration capacity that also allows cooling below ambient temperature. This well-known principle for air conditioning the interior of a car in summer is also used to cool the battery when the outside temperature is very high. The heat released during condensation (transition from gas to liquid) can also be used to heat the interior of the car in winter. The refrigerant circuit is driven by an electric air conditioning compressor, which compresses the refrigerant to the required pressure, allowing evaporation and condensation at selected temperature levels [5]. The main objectives of the paper are to design a model and simulate representative models of fast and ultrafast charging methods and make a comparison between the charging speeds of both methods. Also, design a suitable Thermal management system for the battery to calculate the temperature condition.

There are two main methods of charging electric vehicles: fast charging and ultra-fast charging, with limited outdoor testing in the later stages of development. Well-known supercharger networks use fast charging methods. The most important criterion in the development of charging methods is the improvement of charging speed. Therefore, in this paper, the details of a virtual model simulation that achieves the publicly known charging speed promised by the ultra-fast charging method under development and compared with other models are presented. The ultrafast charging method is compared to a similar model simulating the charging speed of the fast charging method for electric vehicles. The corresponding thermal management system is also simulated in detail in the final part of the work, as increasing the charging power also increases the heat generation of the battery.

2. Dynamic Wireless Charging System and Its Components

The dynamic electric vehicle wireless charging system represents an upcoming charging method called ultra-fast charging, while the legacy model represents an existing commercially popular method called fast charging under brand names like Supercharger. Both the models are used for simulation in MATLAB Simulink and compare their outputs to compare the difference in load times [6]. DWC technology enables seamless charging of electric vehicles, effectively extending vehicle range and reducing waiting times for parking lot charging. In the DWC method, since the conductor rail is buried underground [7], it cannot be changed after construction. Since different vehicle types (cars, buses, etc.) have different output voltage and output power requirements, the on-board receiver must be individually designed to allow different vehicles to be applied to a common power rail. Mutual inductance, the most important factor that directly determines output power, depends on many parameters such as receiver position and construction. Therefore, mutual inductance calculation and the relationship between mutual inductance and receiver parameters are key points in the receiver design process. Figure 2.1 shows the working dynamic wireless charging system.

Fig 2.1: - Diagram showing the working of a dynamic wireless charging system

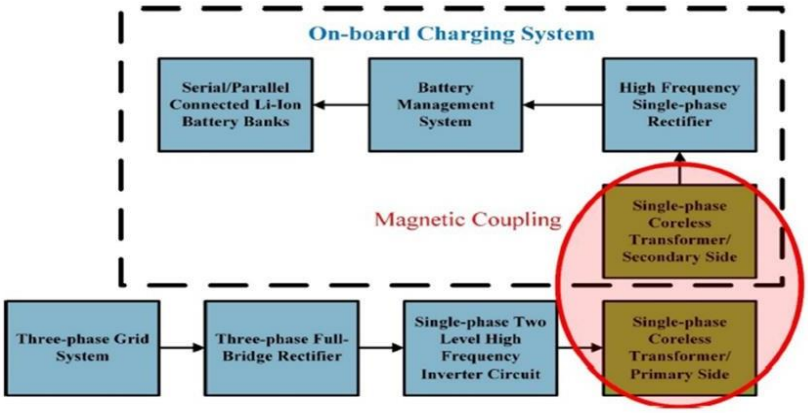

The power supply of the charging station is the AC-DC converter circuit. A DC voltage is converted to a high-frequency AC voltage at the desired amplitude with a phase two-level inverter circuit at the output of this design. Then the high-frequency AC voltage induced on the vehicle side secondary winding is rectified and the DC voltage is connected to the battery charge control system. The road infrastructure of the dynamics wireless charging system is shown in figure 2.2.

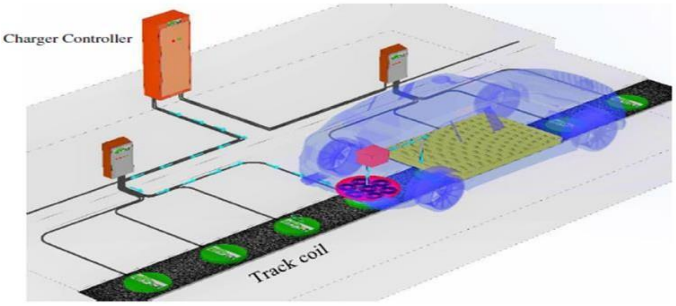

Fig 2.2: - Diagram showing road infrastructure of a dynamic wireless charging system

3. Calculation of Coupling Coefficient between the Transmitter and Receiver Coils

As shown in Figure 3.1, when the receiving coil is placed above the transmitting coil at a height '*h*', the coupling coefficient κ between the coils is proportional to the ratio of the overlapping area of the coils to the area of the transmitter coils and inversely proportional to the cube of the distance between the coils [8]. In this study for $b < 2R$, k can be estimated using the following formula:

$$\kappa = \frac{2R}{a} \cdot \left(\frac{R}{\sqrt{b^2+4h^2}}\right)^3 \quad (1)$$

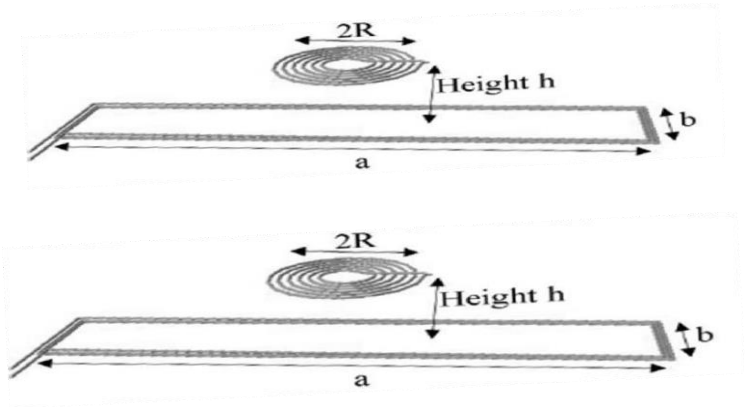

Fig 3.1: - Diagram showing transmitter and receiver coils

By using longer transmission coils, less power electronics and compensation circuits are required for the same length of road, thus reducing the cost per route unit of infrastructure. However, from the above equation it can be found that the coupling coefficient κ decreases as the transmitter coil length increases. i.e., larger '*a*', smaller 'κ' results in lower power transfer efficiency η and also, the lower the power that the system can transmit. Theoretically, the maximum power transfer efficiency η of the system can be calculated by analyzing the circuit shown in Figure 3.2 as follows.

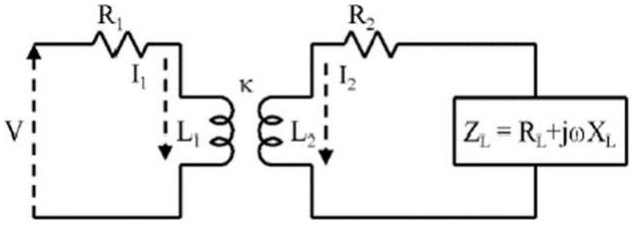

Fig 3.2:- Circuit diagram of transmission and receiver coils

$$\eta = \frac{I_2{}^2 R_L}{I_1^2 R_1 + I_2^2 R_2 + I_2^2 R_L} = \frac{R_L}{\frac{(R_2+R_L)^2+(\varpi L_2+X_L)^2}{(\varpi M)^2} R_1 + R_2 + R_L} \quad (2)$$

$$\therefore \eta_{\max} = \frac{1}{1+\frac{2}{\kappa^2 Q_1 Q_2}+2\frac{\sqrt{\kappa^2 Q_1 Q_2+1}}{\kappa^2 Q_1 Q_2}} \quad (3)$$

The theoretical maximum power transfer efficiency $\eta_{\max}$ shown in Eq. (3) can be obtained only by applying a proper load given by the following equation.

$$R_{L\,\mathrm{m}} = R_2\sqrt{1+\kappa^2 Q_1 Q_2}$$
$$X_{L\,\mathrm{m}} = -\omega L_2$$

The simulated models for both charging methods consist of two parts. The secondary contains the secondary coil for inductive charge transfer along with the battery and the battery management system and remains constant for both models as it is part of the electric vehicle.

Key parts of the fast-charge simulation include a primary coil, a three-phase full-bridge rectifier, and a high-frequency inverter with MOSFETs and PWM control. The ultra-fast charging simulations are almost identical except a boost converter is attached between the three-phase full bridge rectifier and high-frequency inverter to boost voltage levels for faster charging.

List of Symbols and Abbreviations

T = inner cell temperature (ºC)

Ta = ambient temperature (ºC)

RT =convection resistance (W1 m-2 K-1)

CT =heat capacitance (J m-3 K-1)

Ps =power dissipated inside the cell (W)

EV=Electric Vehicle

Vo =Voltage

Io= Current

t= Time

3.1 Working of the Boost Converter

A boost converter is considered a constant current input source because the input current is constant due to the inductance associated with the input source. Also, the load can be viewed as a constant voltage source. A controlled switch turns on and off using pulse width modulation (PWM). PWM can be time-based or frequency-based. The boost converter has two modes of operation. The first mode is when the switch is on and

conducting.

3.2 Calculation of Output Voltage of a Boost Converter

Considering that output current is varying linearly, the energy input provided by the sourceto the inductor, when CH is on and is given by

W_{on} = (Voltage across the inductor) (average current through the inductor)T_{on}

$$W_{on} = V_{\text{in}} \left(\frac{i_1 + i_2}{2}\right) T_{on}$$

Further, the energy that the inductor releases to the load when CH is off is given as:

W_{off} = (Voltage across the inductor) (average current through the inductor) T_{off}

$$W_{off} = V_{0ut} - V_{in} \left(\frac{i_1 + i_2}{2}\right) T_{\text{off}}$$

For a lossless system, comparing the two energies, it will be,

$$V_{\text{in}} \left(\frac{i_1 + i_2}{2}\right) T_{\text{on}} = V_{0ut} - V_{\text{in}} \left(\frac{i_1 + i_2}{2}\right) T_{\text{off}}$$

On simplifying,

$$V_{\text{in}}\, T_{on} = V_{0ut} T_{off} - V_{in} T_{off}$$
$$V_{0ut} T_{off} = V_{in} T_{on} + V_{\text{in}}\, T_{off}$$
$$V_{0ut} T_{off} = V_{in}\left(T_{on} + T_{off}\right)$$

Since, $T = T_{\text{on}} + T_{\text{off}}$

Therefore,

$$V_{0ut} T_{off} = V_{\text{in}}\, T$$
$$V_{0ut} = V_{\text{in}} \frac{T}{T_{\text{off}}}$$
$$V_{0ut} = V_{\text{in}} \frac{T}{T - T_{on}}$$
$$V_{0ut} = V_{in} \frac{1}{\left(\frac{T}{T} - \frac{T_{on}}{T}\right)}$$

Since, Duty cycle i.e., $\alpha = T_{\text{on}} / T$

$$V_{0ut} = V_{\text{in}} \frac{1}{(1 - \alpha)}$$

Thus, it is observed that the average load voltage can be stepped up with the change in the duty cycle.

4. Thermal Management System

The value of the ECM components depends on SOC and inner cell temperature. The inner cell temperature is assumed to be uniform, and taken as the average temperature inside the cell [9]. This cell temperature can be computed by solving the heat equation of a homogeneous body exchanging heat with the environment:

$$C_T \frac{dT}{dt} = -\frac{T - T_a}{R_T} + P_s$$

Applying a Laplace transformation:

$$T(s) = \frac{P_s R_T + T_a}{1 + R_T C_T s}$$

Test Cycle Control

The test cycle was implemented to control the charging, discharging, and measurement systems using the GPIB standard interface and digital I/O of a data acquisition card.

Equivalent circuit model parameters

Each element of the equivalent circuit of pack1 of Figure (4.1) is a function of SOC and temperature. Specifically:

R0= R0(SOC, T)

R1=R1(SOC, T)

C1=C1(SOC, T)

Em= Em (SOC, T)

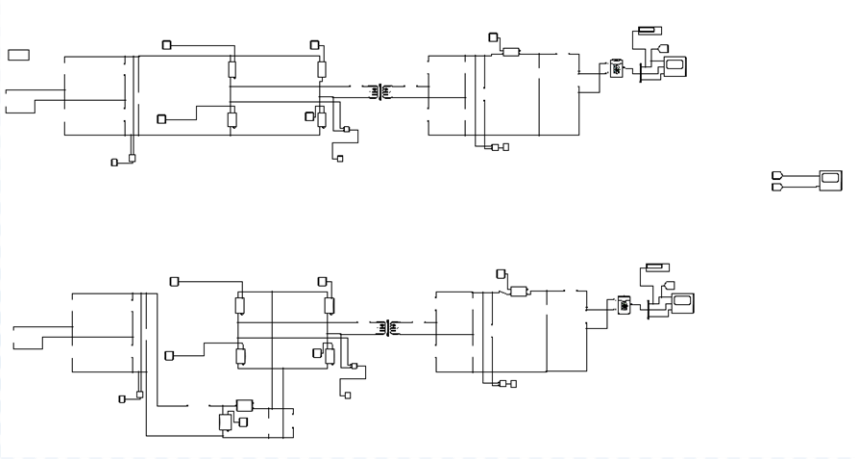

Fig 4.1:- Circuit Diagram for [i] (top) Wireless Fast Charging System and [ii](bottom)Wireless Ultra-Fast Charging System

4.1 Output Waveforms of Charging Systems

Vo

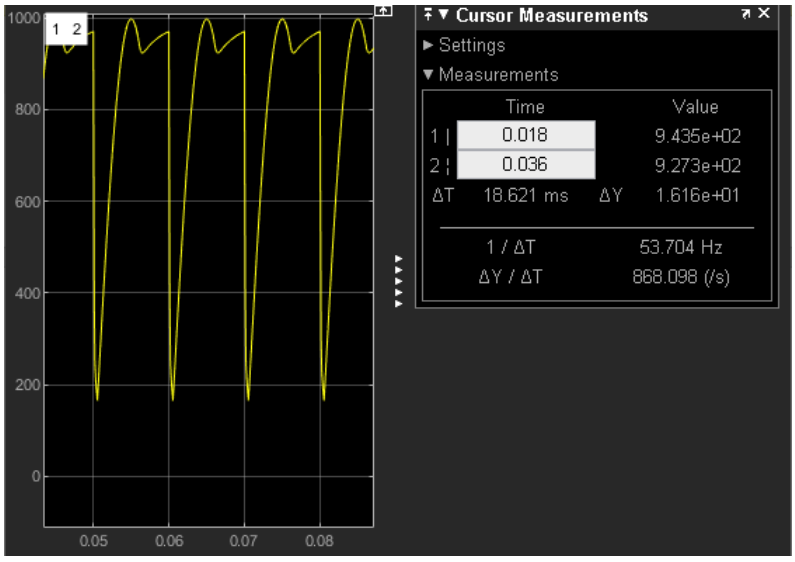

Fig 4.2: - Input Waveform of converter

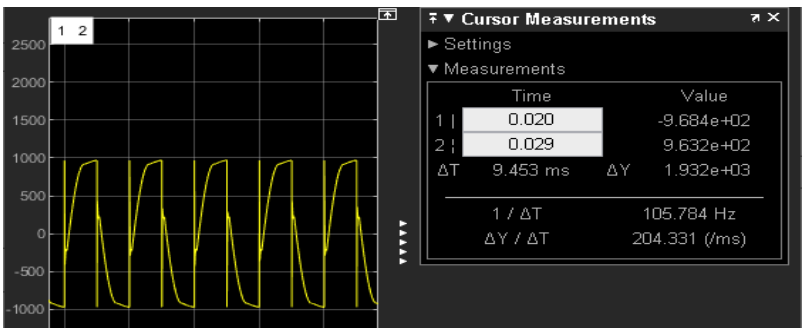

V_o

T(Sec)

Fig 4.3: - Output Waveform of converter

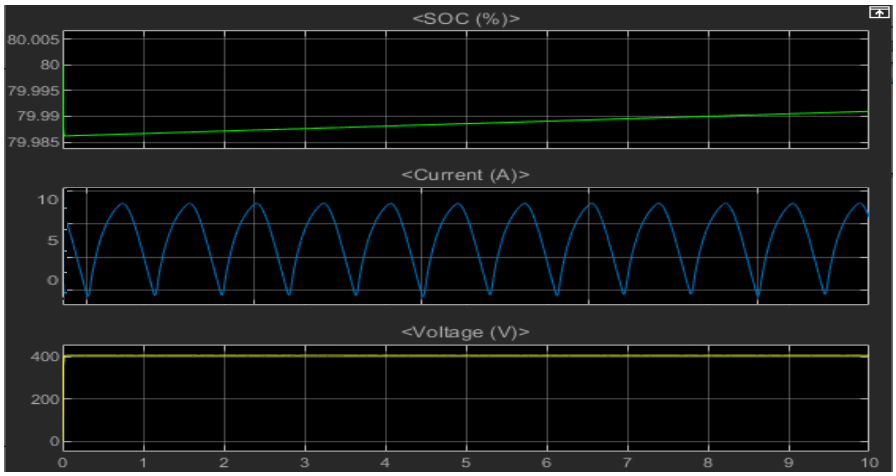

T (sec)

Fig 4.4: - Battery statistics for fast charging simulation

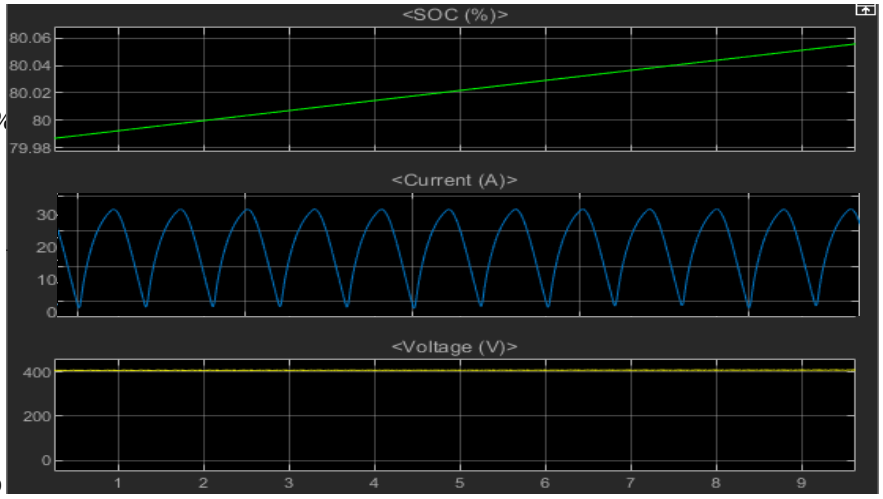

T (sec)

Fig 4.5: - Battery statistics for Ultrafast charging simulation

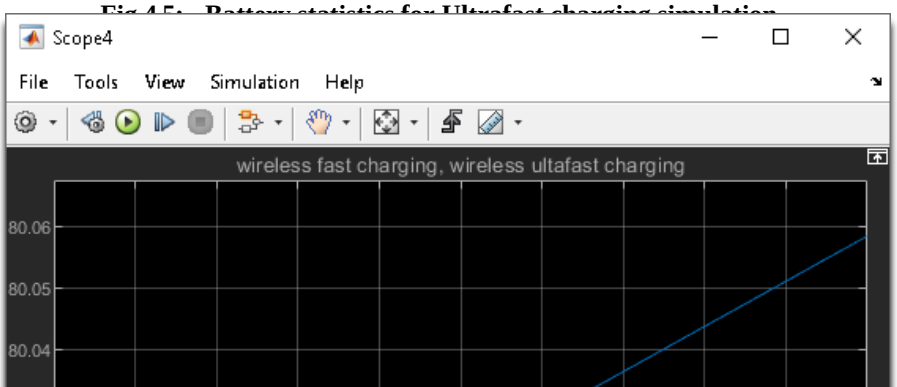

(%)

T (sec)

Fig 4.6: - Side-by-side SOC comparison of fast charging model (green)vs Ultra-fast charging model (blue)

Two wireless charging systems have been manufactured, one of which is fitted with a boost converter on the primary. This is used to create the voltage difference between the two models. A high-voltage model is used to represent an ultra-fast charging system, and another model is used to represent a fast charge, since the charging of a lithium-ion battery depends more on the voltage level than on the current level. Table 1 compares the SOC of both models after a 10 second sampling time from an initial charge of 79.985%.

Table (1): - Voltage and current levels of Fast charging System and Ultrafast Charging system

Model	Voltage(V) at T= 0 sec	Current (A) at T= 0 sec	Voltage(V) at T=10 sec	Current (A) at T=10 sec
Wireless Fast charging	350	0	396	10
Wireless Ultrafast charging	350	0	408	34

5. Circuit Diagram and Simulation Results of Thermal Management System

Fig 5.1: - Circuit Diagram for simulation of Thermal Management System.

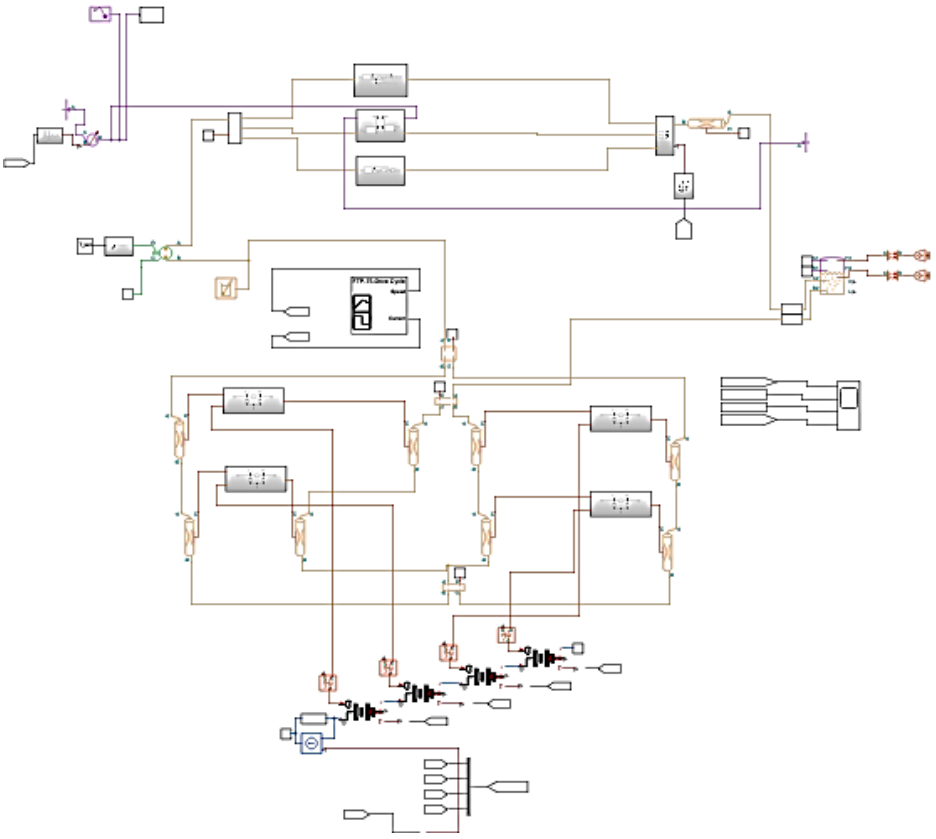

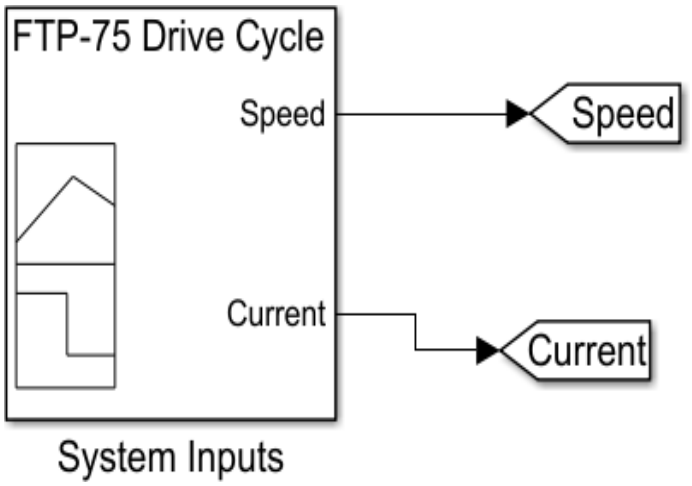

Fig 5.2: - Custom Signal builder block for FTP-75 Drive Cycle

Fig 5.3: - Signal builder view for FTP-75 Drive Cycle

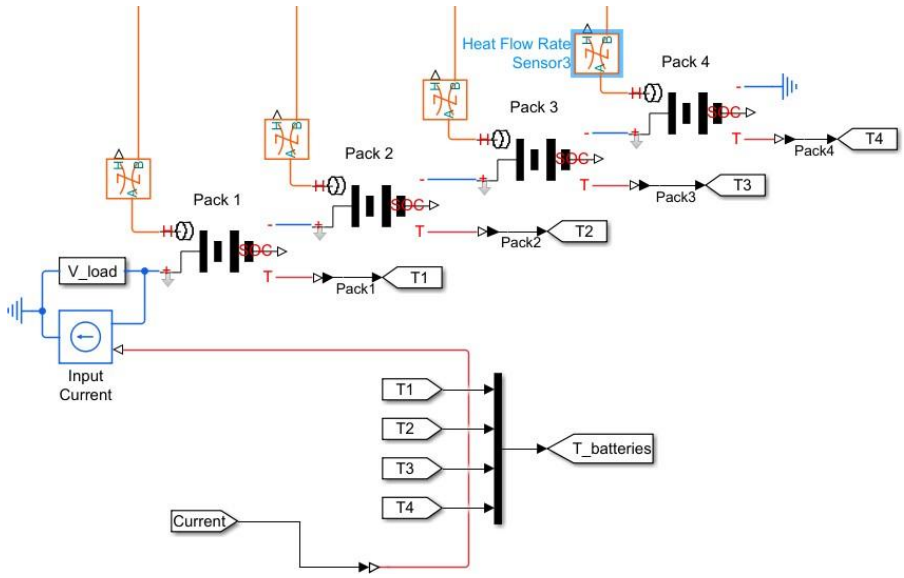

Fig 5.4: - Custom battery Pack for Physical Simulation

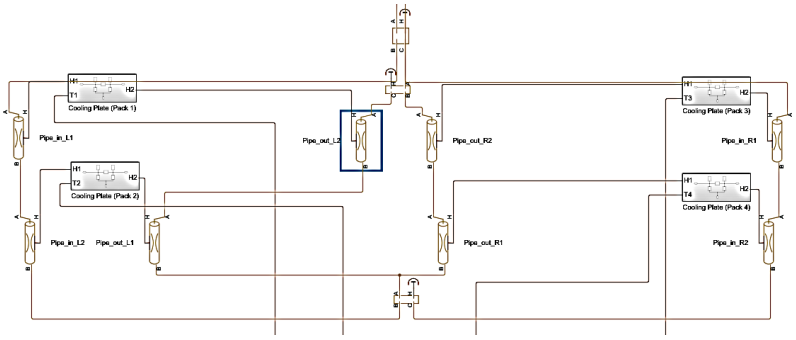

Fig 5.5: - Series of cooling plates with pipes carrying refrigerant around them.

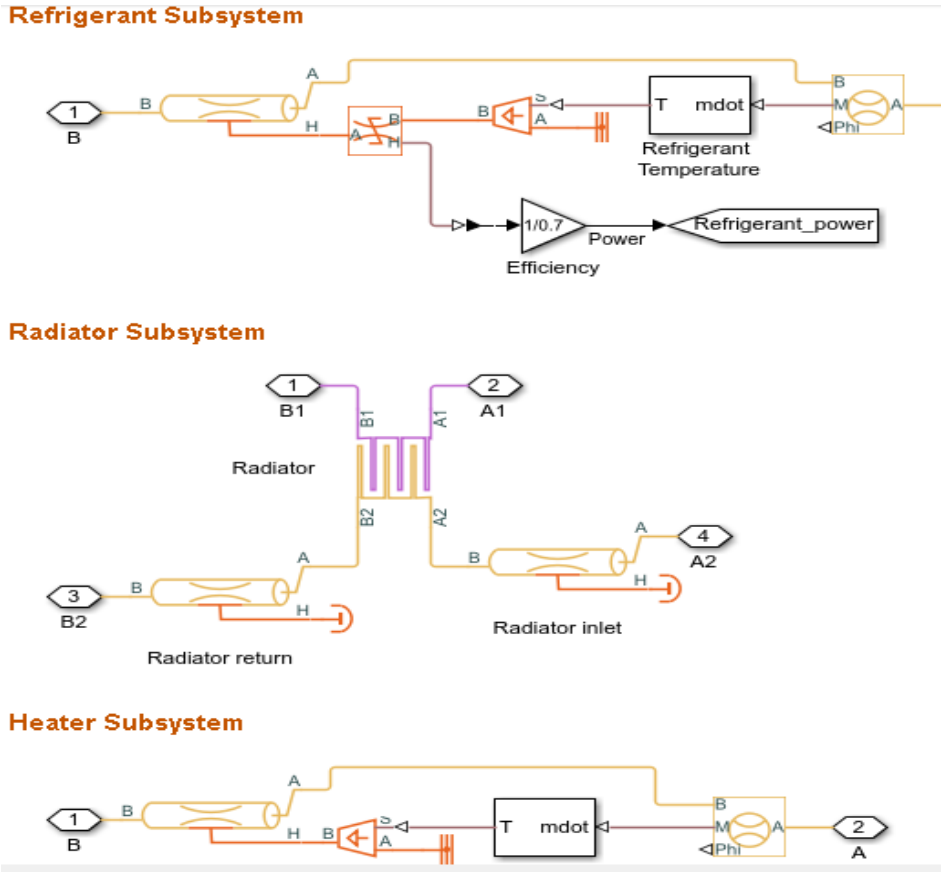

Fig 5.6:- Various subsystems of the Cooling Control Section

5 . 1 Output Waveforms Simulation of Thermal Management System

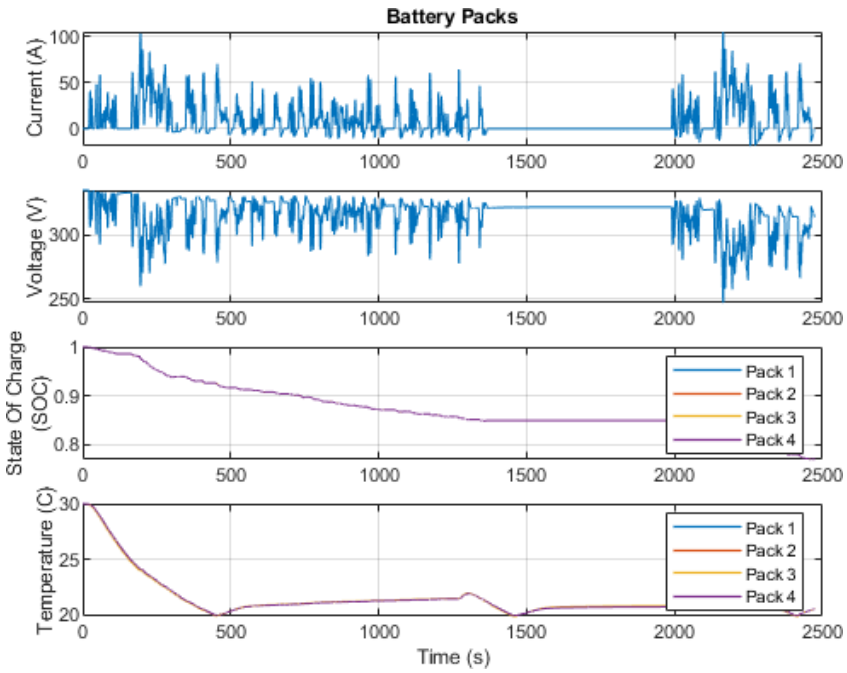

Fig 5.7:- SSC explorer waveforms related to battery

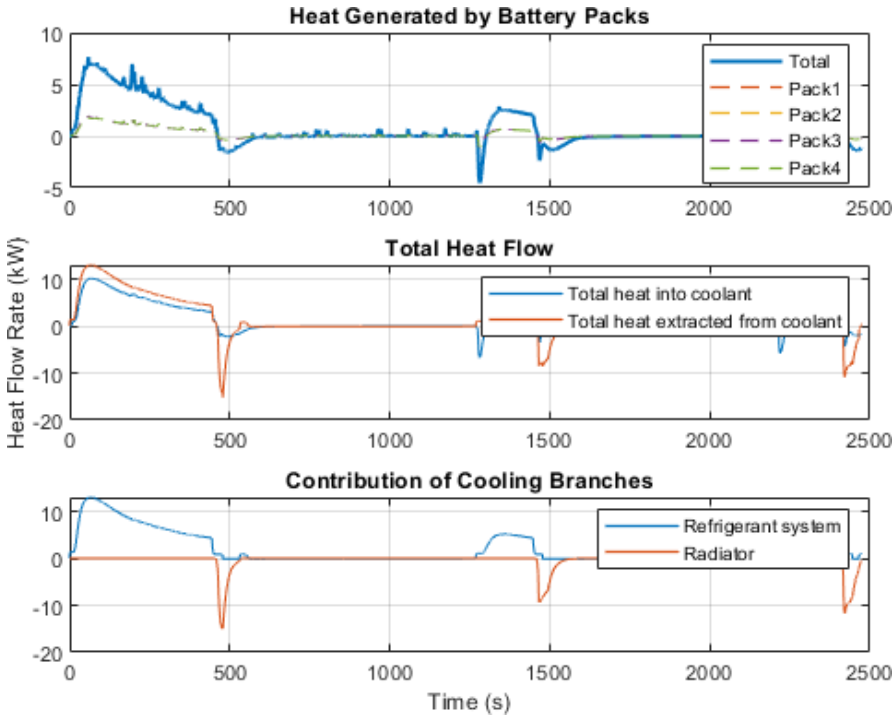

Fig 5.8:- SSC explorer waveforms related to cooling efficiency

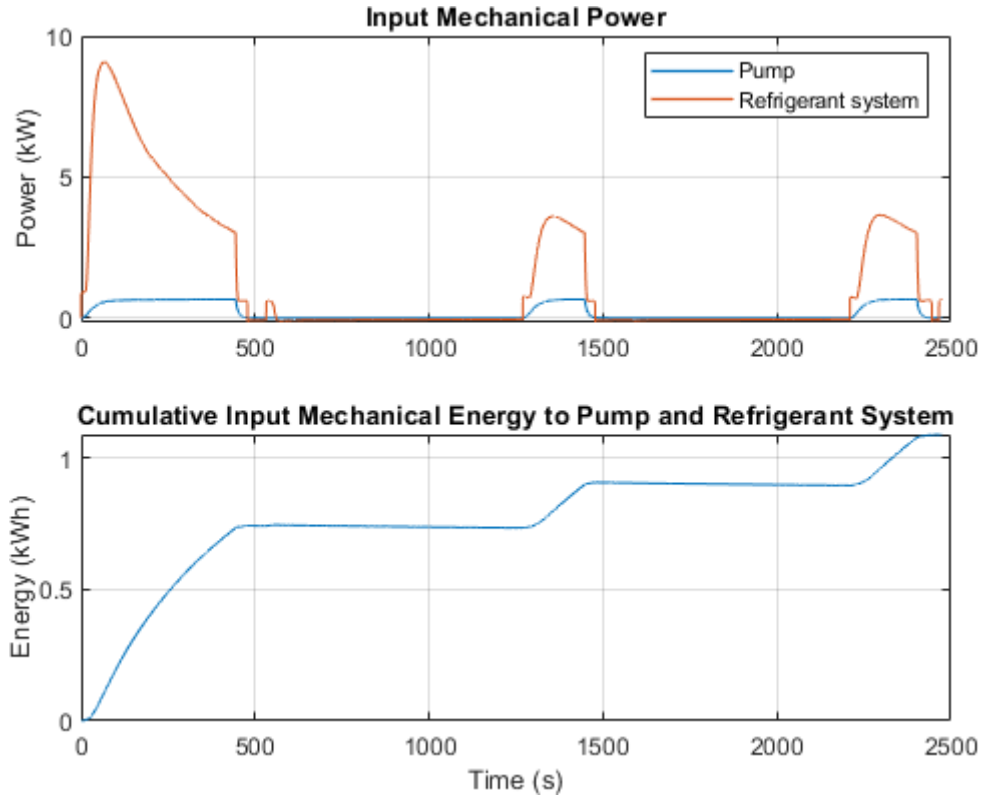

Fig 5.9:- SSC explorer waveforms related to mechanical power flow in a system

The coolant, which is 50-50 ethylene glycol, is pumped into the chiller unit at a set point using a constant displacement pump. Dry air is also pumped using an airflow block connected to a controlled mass flow block for use with radiators.

Heating and cooling units are refrigerant, heater and radiator. The heater warms the frigid battery and the refrigerant unit cools the frigid battery. Radiators, on the other hand, work by using air to maintain temperature under steady operating conditions. Table 3 shows the voltage drop statistics with temperature.

Table 3: - Showing voltage drop with temperature

Time (sec)	T=0	T=1400	T=2500
Temperature(Celsius)	30	23	20
Voltage(v)	325	275	225

The proposed Ultrafast charging system for electric vehicles compared to the commercial fast charging system is shown in Table 4.

Table 4: - Comparative Study between both charging models

State of Charge (%) at T=0 sec	State of Charge (%) at T=10 sec	Model
79.985	79.992	Wireless Fast charging
79.985	80.06	Wireless Ultrafast charging

6. Conclusion

This paper shows a comparison of the two charging systems by analyzing two different charging methods. The graphs between SOC (state of charge) and charging time is obtained for both the fast charging model and the ultra-fast charging model. It is observed that the slope of the ultra-fast charging model is larger than that of the fast charging model. Therefore, with the same charging time, the battery charges more in the ultra-fast charging model.

The thermal management system uses three temperature optimization modes, using 50-50 ethylene glycol as a coolant, not only cools but also maintains temperature, reducing the shortcomings of fast charging systems and improving the future of electric vehicles. The results also show that as the average temperature decreases, the battery discharge rate also decreases and the charge rate increases.

7. References

[1] T. Fujita, T. Yasuda, and H. Akagi, "A dynamic wireless power transfer system applicable to astationary system", *IEEE Trans. Ind. App.*, vol. 53, no. 4, pp. 3748-3757, Aug. 2017.

[2] T. Kan, T.D. Nguyen, J.C. White, R.K. Malhan and C. Mi, "A new integrated method for anelectric vehicle wireless charging system using LCC compensation topology: analysis and design ", IEEE Trans. Power Electron., vol. 32, no. 2, pp. 1638-1650, Feb. 2017.

[3] S. Wang, J. Chen, Z. Hu, and M. Lui, "Study on series-parallel mixed resonance model ofwireless transfer via magnetic resonance coupling", Progress in Electromagnetic Research Symposium (PIERS), pp. 2941-2945, Aug. 2016

[4] M.R. Amin and R.B. Roy, "Design and simulation of wireless stationary charging for hybridelectric vehicle using inductive power pad in parking garage", 8th International Conference on Software Knowledge Information Management and Applications (SKIMA), Dec. 2014.

[5] O. Knecht and J.W. Kolar, "Comparative evaluation of IPT resonant circuit topologies forwireless power supplies of implantable mechanical circulatory support systems", Applied Power Electronics Conference and Exposition (APEC), pp. 3271-3278, Mar. 2017

[6] F. Zhao, G. Wei, C. Zhu, and K. Song, "Design and optimization of asymmetric solenoid typemagnetic coupler in wireless charging system for electric vehicles", IEEE PELS Workshop on Emerging Technologies: Wireless Power Transfer (WoW), pp. 157-162, Apr.

[7] S.D. Barman, A.W. Reza, N. Kumar, M.E. Karim, and A.B. Munir, "Wireless powering bymagnetic resonant coupling: recent trends in wireless power transfer system and its applications", *Renew. Sustain. Energy Reviews*, vol. 51, pp. 1525-1552, Nov. 2015.

[8] Y.P. Su, X. Liu, and S.Y.R. Hui, "Mutual inductance calculation of movable planar coil onparallel surfaces", IEEE Trans. Power Electron., vol. 24, no. 4, pp. 1115-1124, April 2009.

[9] Tarun Huria, Massimo Ceraolo, Javier Gazzarri and Robyn Jackey "High Fidelity Electrical Model with Thermal Dependence for Characterization and Simulationof High-Power Lithium Battery Cells" IEEE, 16 April 2012.

[10] M. Ceraolo, G. Lutzemberger, T. Huria, "Experimentally Determined Models for High-Power Lithium Batteries", Advanced Battery Technology 2011, SAE, April 2011. ISBN: 978-0-7680-4749-3. DOI: 10.4271/2011-01-1365.

[11] Min Chen; G.A. Rincon-Mora, "Accurate electrical battery model capable of predicting runtime and I-V performance," Energy Conversion, IEEE Transactions on, vol.21, no.2, pp. 504-511, June 2006. DOI: 10.1109/TEC.200.